

Source-independent quantum random number generator against detector blinding attacks

Wen-Bo Liu,^{1,*} Yu-Shuo Lu,^{1,*} Yao Fu,^{2,3} Si-Cheng Huang,^{1,4}
Ze-Jie Yin,⁴ Kun Jiang,² Hua-Lei Yin,^{1,†} and Zeng-Bing Chen^{1,3,‡}

¹*National Laboratory of Solid State Microstructures and School of Physics,
Collaborative Innovation Center of Advanced Microstructures, Nanjing University, Nanjing 210093, China.*

²*Beijing National Laboratory for Condensed Matter Physics and Institute of Physics,
Chinese Academy of Sciences, Beijing 100190, China*

³*MatricTime Digital Technology Co. Ltd., Nanjing 211899, China*

⁴*State Key Laboratory of Particle Detection and Electronics,
University of Science and Technology of China, Hefei 230026, China*

(Dated: April 27, 2022)

Randomness, mainly in the form of random numbers, is the fundamental prerequisite for the security of many cryptographic tasks. Quantum randomness can be extracted even if adversaries are fully aware of the protocol and even control the randomness source. However, an adversary can further manipulate the randomness via detector blinding attacks, which are hacking attacks suffered by protocols with trusted detectors. Here, by treating no-click events as valid error events, we propose a quantum random number generation protocol that can simultaneously address source vulnerability and ferocious detector blinding attacks. The method can be extended to high-dimensional random number generation. We experimentally demonstrate the ability of our protocol to generate random numbers for two-dimensional measurement with a generation speed of 0.515 Mbps, which is two orders of magnitude higher than that of device-independent protocols that can address both issues of imperfect sources and imperfect detectors.

I. INTRODUCTION

The unpredictability of random numbers was originally intended to refer to a lack of correlation between numbers. However, pseudorandom numbers [1, 2] and true random numbers [3, 4] are obtained through deterministic formulas and dynamics, respectively, implying some correlation of these numbers and, hence, some predictability of subsequent numbers. In contrast, quantum random numbers [5, 6] are considered to have inherent randomness based on the completeness of quantum mechanics. Quantum random number generators (QRNGs) have thus been widely investigated to obtain unpredictable random numbers. In addition to their lack of correlation, the practical security of quantum random numbers has received considerable attention as their fields of application [7–9] expand to cryptographic tasks [10–14].

As a solution to almost all security concerns, device-independent QRNGs [15–18] are the most stringent, making no assumption about either randomness sources or detection devices. Recently, device-independent QRNGs that can extract random numbers after deducting the consumed randomness have been implemented for the first time. The net gains reached 2290 bps [19], 3606 bps [20] and 3718 bps [21]. However, they all required approximately 10 hours to accumulate data, which would

lead to high latency in practical use. Furthermore, random numbers are consumed rapidly in most cryptographic tasks. Thus, we unavoidably consider the trade-off between the security and the generation rate [22–24]. An adoptable choice is the source-independent QRNG (SI-QRNG) [25–30], in which the detection devices are assumed to be trusted, unlike in device-independent

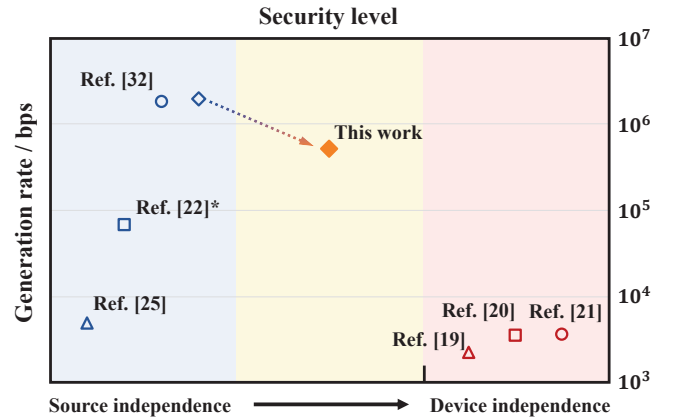


FIG. 1. Security levels and generation rates in discrete-variable QRNG experiments. Improved security usually comes at the expense of a lower generation rate. Being immune to detector blinding attacks, our protocol has a significantly higher security level than source-independent protocols. It bears emphasizing that the left-right order of markers in the same color represents only the generation rate, not the security level. *It may have higher security than previous source-independent protocols, but it still cannot resist detector blinding attacks.

* These authors contributed equally to this work

† hlyin@nju.edu.cn

‡ zbchen@nju.edu.cn

QRNGs.

Unfortunately, since an adversary (Eve) can emit arbitrary signals into detectors, the detection component is more vulnerable to quantum hacking attacks than the source [31]. To guarantee the security of detection, detection devices should be carefully characterized to evaluate device imperfections [32, 33]. However, detector blinding attacks [34–36], the most powerful attack targeting detectors, have not yet been efficiently solved. In detector blinding attacks, Eve manipulates the detector using trigger light with specific optical power and determines the detection outcomes with a probability of almost 100%. Such attacks can be launched on either avalanche photodiodes [37] or superconducting nanowire single-photon detectors [38].

There are several experimental countermeasures against detector blinding attacks. A common solution is to install a beam splitter before signals enter the detection equipment to monitor the light intensity [39]. Crafty adversaries can instead send instantaneous bright trigger light, which blinds the detector without disrupting the monitor [35, 36]. Other solutions [40–43], such as randomly changing the attenuation in front of the detector and analyzing the corresponding detection events and errors, also increase the difficulty of experimental operation [44]. While experimental solutions attempt to judge whether the generator is under attack by designing a more sophisticated system, further advanced attacks from Eve usually cannot be avoided [44, 45]. Therefore, it is vital to develop theoretical approaches that can fundamentally address detector blinding attacks.

Inspired by the interpretation of no-click events in Bell tests [46], we find that the fair sampling assumption is broken in the presence of detector blinding attacks, and that no-click events should be valid events. In this work, we present a source independent protocol abandoning the assumption that the detectors work properly, thus it is secure against detector blinding attacks. Our protocol has composable security against quantum coherent attacks, and can be easily expanded to high-dimensional measurement cases. We experimentally demonstrate the feasibility of generating random numbers in the two-dimensional measurement case. Our protocol achieves higher security than previous SI-QRNGs and maintains a meaningful generation rate, as shown in Fig. 1. In our experiments, the highest generation rate is 0.103 with 1 Gb of data accumulation. Using a 5 MHz experimental system, we achieve a quantum random number generation speed of over 500 kbps. Considering the needs of low-latency applications, our experimental system is able to generate 640 kbit quantum random numbers every 2 seconds. The extracted quantum random numbers pass the NIST test.

II. DETECTOR BLINDING ATTACKS.

Typically, single-photon detectors are threshold detectors that fire when at least one photon arrives. However,

detector blinding attacks are able to arbitrarily control the threshold of these detectors [34]. We first construct a threshold detection model for detectors under bright illumination. Second, based on this model, we introduce a balanced attack strategy in which the detection thresholds of all detectors are equal. A more complex and powerful attack strategy is also considered in which the thresholds of different detectors are different.

A. Threshold detection model.

As the receiver, Alice detects signals randomly in one of two incompatible bases \mathbb{X} and \mathbb{Z} . Without loss of generality, we agree that the outcomes in \mathbb{Z} are used to generate raw random numbers and the outcomes in \mathbb{X} are used to judge the amount of information obtained by Eve. In the two-dimensional measurement scheme, we notate the eigenstates of \mathbb{Z} as $\{|0\rangle, |1\rangle\}$, and the eigenstates of \mathbb{X} as $\{|\pm\rangle = \frac{1}{\sqrt{2}}(|0\rangle \pm |1\rangle)\}$. When the \mathbb{X} basis is chosen, the outcome $|+\rangle$ is considered the correct outcome, and the outcome $|-\rangle$ is an error event [25].

If the threshold of a detector is an intensity I , the detector fires when the intensity of the signal is stronger than I and does not fire when it is equal to or weaker than I . In the detector blinding attack scenario, Eve can arbitrarily determine the value of I by exploiting the tailored bright illumination, and Alice cannot obtain this value unless additional monitoring is performed. Under the active-basis-choice, we can assume that the threshold of the detector representing $|0\rangle$ and $|+\rangle$ is $I_0 = I_+$ and that the threshold of the detector representing $|1\rangle$ and $|-\rangle$ is $I_1 = I_-$. $I_0 = I_1 = 0$ when Eve sends signals without bright illumination. When Eve sends signals with bright illumination, the thresholds of the different detectors can be arbitrary.

B. Attack with $I_0 = I_1$.

We start with a balanced attack in which Eve adjusts the detectors to have the same threshold I_{th} , as shown in Fig. 2a. Eve wants Alice to obtain an outcome specified by Eve when Alice measures the signal in \mathbb{Z} . In other words, a signal with intensity $I_e > I_{th}$ enters either the detector representing $|0\rangle$ or the detector representing $|1\rangle$ in accordance with Eve's arrangement. Here, we assume that the detectors have perfect efficiency. At the same time, Eve requires the detectors not to fire if Alice happens to measure the signal in \mathbb{X} . Since half of the photons in the signal arrive at the $|+\rangle$ detector and the others arrive at the $|-\rangle$ detector, Eve sets $0.5I_e \leq I_{th}$ to cause a no-click event. In squashing models [47–49], no-click events are treated as receiving vacua and thus are discarded without increasing the error count. Therefore, by emitting signals with $I_{th} < I_e \leq 2I_{th}$, Eve can control the outcomes of \mathbb{Z} -basis measurements without increasing the error rate in \mathbb{X} .

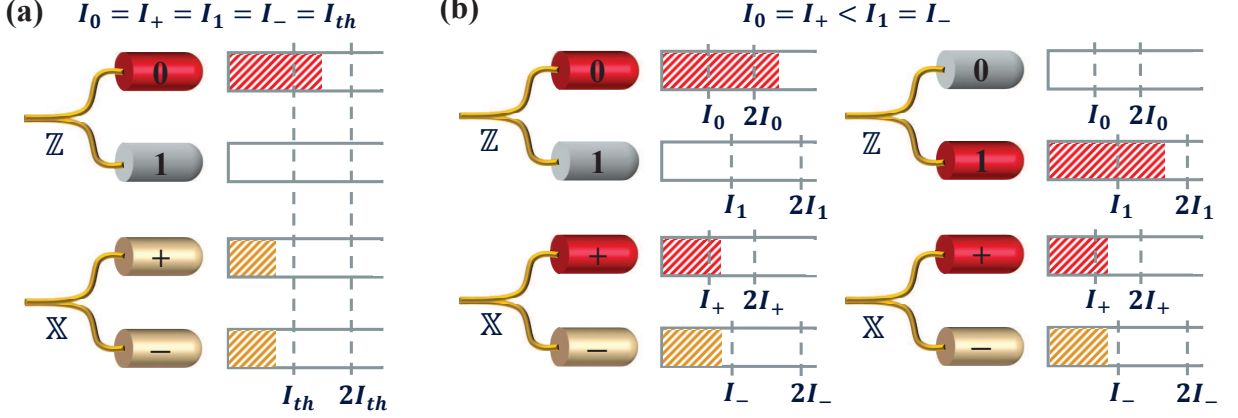


FIG. 2. Detector blinding attacks. (a) The case in which both detectors have the same thresholds. Although Eve controls the outcomes of measuring signals in \mathbb{Z} , both detectors do not fire if Alice happens to measure signals in \mathbb{X} . (b) The case in which the detector representing $|+\rangle$ has a lower threshold than the other. When Eve controls the outcomes of measuring signals in \mathbb{Z} , she can also cause the detector representing $|+\rangle$ to fire if Alice happens to measure signals in \mathbb{X} .

C. Attack with $I_0 \neq I_1$.

As shown in Fig. 2b, the thresholds of the different detectors are different. A more favorable option for Eve is $I_+ < I_-$ since $|+\rangle$ represents the correct outcome. For the active-basis-choice, we have $I_0 = I_+$ and $I_1 = I_-$, which means that $I_0 < I_1$. In this case, Eve can cheat both bases at the same time, i.e., she controls the outcomes in \mathbb{Z} while ensuring that only the $|+\rangle$ detector fires in \mathbb{X} . If Eve wants Alice to obtain an outcome of $|0\rangle$, she emits a signal with $I_e > I_0$, and all photons in it are sent to the $|0\rangle$ detector under the \mathbb{Z} basis. If Eve wants Alice to obtain an outcome of $|1\rangle$, she emits the signal with $I_e > I_1$, and all photons in it are sent to the $|1\rangle$ detector under the \mathbb{Z} basis. To make the outcomes in \mathbb{Z} credible, she also requires $0.5I_e \leq I_-$ and $0.5I_e > I_+$ under the \mathbb{X} basis. Overall, the intensity of the signal should be $\max\{I_1, 2I_0\} < I_e \leq 2I_1$, which does not violate the premise $I_0 < I_1$. Therefore, Eve has an absolutely dominant strategy.

D. d -dimensional case.

Detector blinding attacks also work in the d -dimensional measurement scenario. Two measurement bases \mathbb{X} and \mathbb{Z} are both d -dimensional and ideally have the relation $|\langle z|i|j\rangle_x| = 1/\sqrt{d}$ between any eigenstate $|i\rangle_z$ ($i \in \{1, 2, \dots, d\}$) of \mathbb{Z} and any eigenstate $|j\rangle_x$ ($j \in \{1, 2, \dots, d\}$) of \mathbb{X} . The outcome $|0\rangle_x$ is the correct outcome in \mathbb{X} . Eve will emit signals with intensity $I_{th} < I_e \leq dI_{th}$ if she adopts the balanced attack strategy. The situation will be slightly more complicated if Eve wants to control both bases perfectly. She can adjust the threshold of the detector representing $|0\rangle_x$ to the low-

est among all detectors' thresholds. The light intensity should be d times higher than the threshold of the $|0\rangle_x$ detector. To avoid multiple-click events in \mathbb{X} , the light intensity should also be less than d times the sub-smallest threshold. This, in turn, constrains the thresholds of the other detectors to be less than d times the sub-smallest threshold.

III. DEFENSIVE STRATEGY.

In general, Eve controls the detectors while causing no click in the \mathbb{X} basis, which is a hint for us. In terms of this hint, we should reconsider what no click means. First, we briefly review the concept of squashing models and analyze why this hint has been ignored in previous works. Then, we introduce a strategy for handling this hint. The uncertainty relation of smooth entropy is used as a critical tool for generating quantum random numbers that are secure against general attacks. Finally, we generalize the security analysis to the d -dimensional case.

A. Squashing model.

The dimension of the signals output from the channel is unknown since the channel is controlled by Eve. However, the security analysis is usually qubit-based for two-dimensional measurements by virtue of simplicity. The squashing model [47–49] is developed to resolve this conflict. A squashing operation is applied to the signal, which virtually maps the signal into a qubit. A virtual qubit measurement on this virtual qubit follows. Therefore, the qubit-based security analysis is applicable.

Measuring a qubit yields one of two outcomes corresponding to its two eigenstates. However, an unknown signal subjected to two-dimensional measurement actually yields one of four outcomes: a single click in one detector, a single click in the other detector, a double-click or no click. To reconcile this difference in outcomes, there are three treatments for different outcomes of signals. Single-click events in either detector are naturally related to the outcomes of measuring qubits. Double-click events are valid events but tell us nothing about randomness. They are used to evaluate the upper bound of the error rate [48]. Note that another squashing model [47, 49] randomly assigns values for double-click events, and thus has a lower error rate and higher randomness consumption. No-click events are regarded as vacua after losses. The positions of the losses in both bases are assumed to be uniformly random. Under this assumption, there are no qualms about discarding no-click events without disturbing the error rate.

However, detector blinding attacks break this confidence since the thresholds of the detectors can be changed such that a signal can definitely cause clicks in one basis and no click in the other. In the worst case, all no-click events in \mathbb{X} are caused by detector blinding attacks. Therefore, squashing models fail under such attacks.

B. Security analysis.

The key point of our security analysis is how to securely deal with no-click events. Tasks such as Bell tests and device-independent quantum key distribution also suffer from the loophole introduced by no-click events, called the fair sampling loophole. An ingenious method is presented in Bell tests [46], in which some no-click events are retained to close this loophole; otherwise, the experimental results may have been screened by unknown factors. Inspired by this idea, we retain all no-click events. No-click events should have the same status as double-click events since they both have no randomness and can cover up attacks. Therefore, we treat no-click events in the same way as double-click events. They are error events in the \mathbb{X} basis and correct events in the \mathbb{Z} basis, as described in the Appendix section.

As mentioned above, there exists a dominant strategy in which the outcomes in \mathbb{Z} are controlled by Eve, while the outcomes in \mathbb{X} are only single-click events on the $|+\rangle$ detector. In response to this situation, the $|+\rangle$ detector should be randomly assigned by Alice. Eve thus cannot accurately forecast it and has at most a 50% chance of firing in the $|+\rangle$ detector. Since we need only a small percentage of rounds to measure \mathbb{X} , the consumption of random numbers for deciding which detector will be used to measure $|+\rangle$ in each round is not an unbearable burden.

Our security analysis adopts the uncertainty relation of smooth entropy [50, 51] to offer security against the

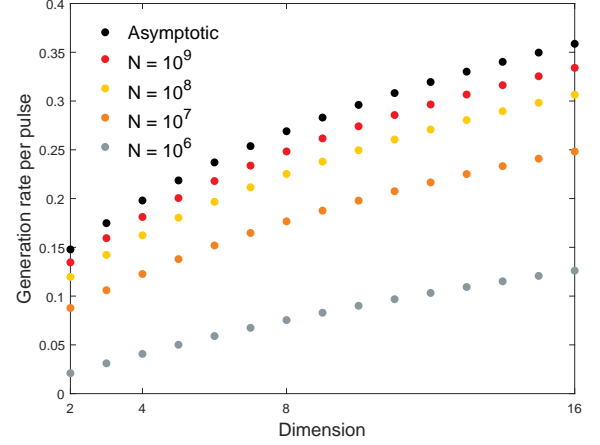


FIG. 3. Dimensions of the measurement basis and generation rates per pulse. The asymptotic case is investigated, in which the amount of data is infinite. Scatter points in different colors represent cases in which the numbers of emitted pulses N are 10^9 , 10^8 , 10^7 and 10^6 .

most general attacks. This relation involves three parties, namely, the user Alice, the virtual user Bob and the adversary Eve, and is expressed as

$$H_{\min}^{\epsilon}(\mathbf{Z}_A|\mathbf{E}) + H_{\max}^{\epsilon}(\mathbf{X}_A|\mathbf{B}) \geq q, \quad (1)$$

where \mathbf{X}_A (\mathbf{Z}_A) means that Alice measures her system A in the \mathbb{X} (\mathbb{Z}) basis. The bound q is an evaluation of the “incompatibility” of the measurement bases \mathbb{X} and \mathbb{Z} . The smooth min-entropy $H_{\min}^{\epsilon}(\mathbf{Z}_A|\mathbf{E})$ is Eve’s minimum uncertainty about \mathbf{Z}_A , which quantifies how much randomness can be extracted. The smooth max-entropy $H_{\max}^{\epsilon}(\mathbf{X}_A|\mathbf{B})$ is related to the error rate of Bob guessing the value of \mathbf{X}_A . Ideally, measuring the signal in the \mathbb{X} basis leads to $\mathbf{X}_A = |+\rangle$. Bob thus can guess $\mathbf{X}_A = |+\rangle$ to obtain a higher random number generation rate if Eve abandons her attack. The specific calculation of these parameters is shown in the Appendix section.

C. d -dimensional case.

We can extend the security analysis against detector blinding attacks to the d -dimensional measurement scenario. In d -dimensional measurement, the squashing model will squash the input signal into a qudit. There are d possible outcomes when one measures the qudit in any qudit basis. The possible real outcomes of signals are no-click events, multiple-click events, and d kinds of single-click events. Single-click events are naturally related to the qudit measurement outcomes. The first two types of events are considered error events in \mathbb{X} -basis measurement and correct events in \mathbb{Z} -basis measurement. To avoid attacks in the dominant strategy case, Alice similarly needs to randomly select the $|0\rangle_x$ detector.

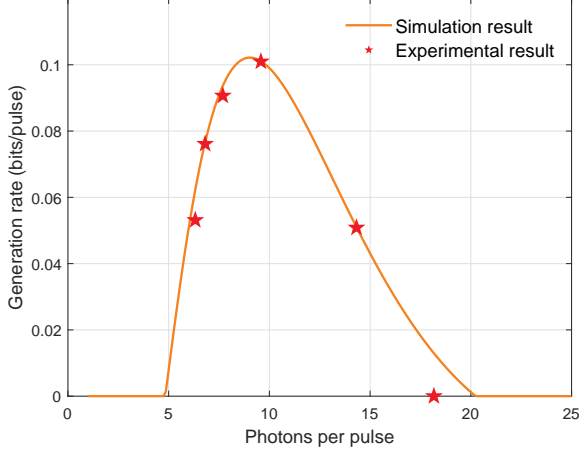


FIG. 5. Random number generation rates in experiments. The orange line represents the simulation results, and red stars represent the experimental results. In the experiment, the random number generation rate is 0.101 when the intensity is $\mu = 9.6$. With 5 MHz system repetition, we accumulate data for approximately 200 seconds at each point, corresponding to a data size of 10^9 , and a random number generation speed of 505 kbps is achieved.

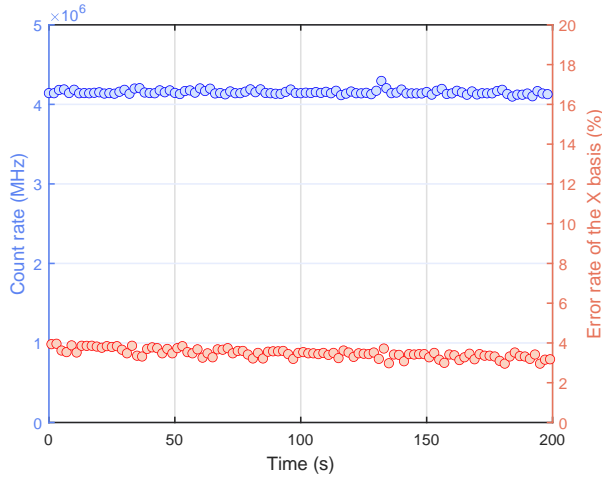


FIG. 6. The detector count rate and error rate over 200 seconds. We use data for a 10 dB channel loss with optimal intensity. Each dot corresponds to the data acquired over two seconds. During testing, the count rate is always approximately 4.15 MHz. No-click events, incorrect detector click events and double-click events are all treated as errors in the \mathbb{X} basis, and the error rate of the \mathbb{X} basis is always less than 4%, which shows the stability of our experimental system.

the source enter the circulator and are fully transmitted through a polarization beam splitter (PBS). The pulses are split by a 45° -aligned polarization beam splitter (45° PBS) and enter a Sagnac interferometer. In the Sagnac interferometer, a phase modulator (PM) driven by an arbitrary waveform generator is utilized to re-

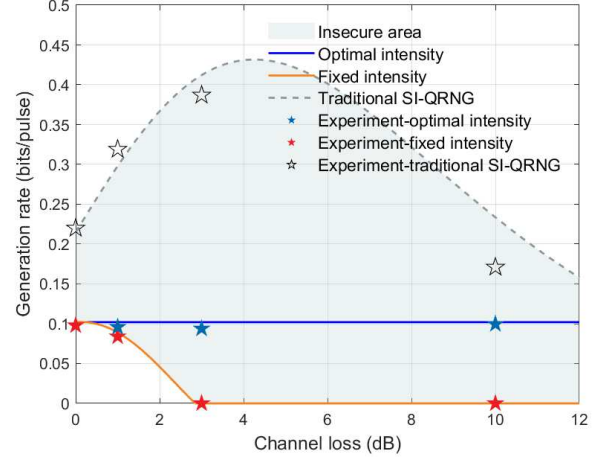


FIG. 7. Relation between the random number generation rates and the channel loss. The blue line is the generation rate when the intensity is always optimal, and the red line is the generation rate when the intensity has a fixed value of $\mu = 9.3$. The gray dashed line is the generation rate of the traditional SI-QRNG protocol with no-click events discarded provided in the Appendix. Stars in different colors represent the experimental results. Discarding no-click events leads to security risks under bright illumination, as shown in the gray filled area.

alize the active-basis-choice by modulating the relative phase between clockwise and anticlockwise propagating pulses. The anticlockwise propagating pulses arrive at the PM with a 25 ns delay relative to clockwise propagating pulses, although they pass through the same fiber. The selections of the measurement basis and the detector representing $|+\rangle$ are commanded by quantum random numbers generated from a previous quantum key distribution experiment [54]. The probability of selecting the \mathbb{Z} basis is 99.95%. When the \mathbb{Z} basis is chosen for measurement, the PM adds a $\pi/2$ phase shift on the earlier arrived pulse. When the \mathbb{X} basis is chosen, to avoid the attack with $I_0 \neq I_1$, PM randomly adds a 0 or π phase shift on the pulse, where the choice of the phase shift determines the detector representing $|+\rangle$. The two pulses are recombined into one in the 45° PBS. After exiting the Sagnac interferometer, the pulse is split by the PBS. Two channels of a superconducting nanowire single-photon detector (SNSPD), D_H and D_V , with detection efficiencies of 49% and 39 %, are utilized to detect the signals that leave the circulator and the PBS, respectively. When the insertion loss of the circulator (1.05 dB) is considered, the detection mismatch is reduced to approximately 0.5%. The dark count rates of the two SNSPD channels are 24 cps and 5 cps, respectively, and the dead time is 50 ns. The detection efficiency of the SNSPD is time-independent. Thus, it is immune to the time-shift attack [55]. The afterpulse issue [33] can also be avoided due to the use of the SNSPD. In our data analysis, all detection events from the entire time period

are used in phase error rate estimation instead of using the preset time window. This strategy enables our experimental system to resist dead time attacks [56].

The randomness source can theoretically be offered by any other party. To demonstrate the ability to generate random numbers with our protocol, we desire $|H\rangle$ pulses to achieve the best generation performance according to the design of our detection equipment. Thus we use the uncharacterized light emitted by a 14-pin butterfly laser diode with a homemade driving circuit and pump it into the slow axis of the polarization maintaining fiber. The laser is triggered by the arbitrary waveform generator and emits pulses with a 5 MHz repetition rate. The best scenario is when the output state of the source is $|H\rangle$. If the output state is another polarization state, it affects only the generated randomness per pulse. The security analysis provided here universally fits the unknown input state.

The intensity of the pulse influences the type of click event and thus affects the generation rate. In Fig. 5, the abscissa represents the light intensity, and the ordinate represents the generation rate. The orange line represents the simulation results, and the red pentacles are the experimental results. For each data point, we collect approximately 200 seconds of data, corresponding to a data size of 10^9 . When calculating the error rate in the \mathbb{X} basis, no-click events, single-click events on the incorrect detector, and double-click events are all taken into account. At the optimal point, the intensity of the pulses before entering the detector is 9.3 photons per pulse, and the random number generation rate is 0.101.

We also consider the influence of the channel loss on random number generation. The loss reduces the light intensity reaching the detector, thereby decreasing the generation rate when the source produces pulses with the optimal intensity. Fortunately, our experimental setup enables us to compensate for the channel loss by increasing the intensity of the source. First, to show the stability of the experimental system, the detector count rate and error rate versus time are presented in Fig. 6. We use data collected with a 10 dB channel loss with optimum intensity. During the 200-second test time, the count rate is always approximately 4.15 MHz (corresponding to $\mu = 9.17$ before entering the detector), and the error rate of the \mathbb{X} basis is approximately 3.5% (including both no-click and double-click events). We then experimentally show the relation between the loss and the generation rate under a fixed intensity and variable intensity, as shown in Fig. 7. Our protocol is compared with the traditional source-independent scheme in the Appendix. The difference between the two schemes is whether no-click events are treated as errors. At each channel loss, the data obtained with fixed intensity are analyzed to calculate the key rate for both our protocol and the traditional source-independent protocol. In the case of high channel loss, the generation rate of our protocol is zero due to the high error rate that results from no-click events. Meanwhile, the traditional source-independent protocol can still gen-

TABLE I. The results of the NIST statistical test. To pass the test, two criteria should be satisfied. If we set the significance level at $\alpha = 0.01$, the minimum proportion of sequences that pass a test item is approximately 0.96, except for the random excursion (variant) test, for which the required proportion is 0.952. In addition, the uniformity of the P-value distribution *P-value* τ should be greater than 0.0001. When a test item yields multiple results, the smallest value is reported.

Test name	<i>P-value</i> τ	Proportion	Result
Frequency	0.1538	1.00	Pass
BlockFrequency	0.9357	0.98	Pass
CumulativeSums	0.2023	1.00	Pass
Runs	0.1816	1.00	Pass
LongestRun	0.1626	0.99	Pass
Rank	0.9781	0.98	Pass
FFT	0.5955	0.98	Pass
NonOverlappingTemplate	0.0118	0.99	Pass
OverlappingTemplate	0.4559	1.00	Pass
Universal	0.2493	0.99	Pass
ApproximateEntropy	0.4559	1.00	Pass
RandomExcursions	0.0106	0.984	Pass
RandomExcursionsVariant	0.0022	0.984	Pass
Serial	0.8165	0.99	Pass
LinearComplexity	0.5749	0.97	Pass

erate random numbers, and the generation rate can be as high as 0.387 (corresponding to 1.94 Mbps) when the channel loss is 3 dB. This difference in the generation rate under the same loss reflects the maximal security vulnerabilities caused by detector blinding attacks. By increasing the intensity of the source to compensate for the channel loss, the generation rate can be maintained at the optimal level.

To further verify the quality of the final output random numbers, we apply the standard NIST statistical tests [57]. After collecting data for approximately 200 seconds, a total of 1.02×10^9 pulses have been sent, and the key rate is 0.103. After privacy amplification, the final random number of length 1.05×10^8 is divided into 100 bitstreams, and fifteen statistical tests are implemented. As shown in Table I, the random numbers generated in the experiment pass all NIST statistical tests.

VI. DISCUSSION

In conclusion, we have proposed an SI-QRNG type protocol that can further resist the most powerful detector attack: the detector blinding attack. By exploiting the uncertainty relation of smooth entropy, our protocol can be easily extended to high-dimensional measurement cases with composable security against coherent attacks under the finite-key effect. Bell tests [46] can use the probability correlation of click events to extract only part of the no-click events from the results. Accordingly, our

protocol has the opportunity to reduce the impact of no-click events on the error rate through a certain probability correlation to improve the generation rate.

In our experiments, the detection loss and the channel loss can be compensated by improving the emission intensity. By increasing the saturation count rate of the detectors to GHz [58], the QRNG generation rate can be enhanced to more than 100 Mbps. Through some simple experimental tricks, our experimental implementation suppresses most well-known attacks on detector components, realizing an extremely high security level approaching device-independence.

A passive-basis-choice approach may also help realize random generation. We apply an active basis choice in our protocol, which consumes a considerable amount of random numbers. For this reason, our protocol is a random expansion rather than an absolutely random generation. Passive-basis-choice can avoid this kind of consumption and enables real random extraction through further discarding the double-basis clicks. To maintain security, some assumptions must be introduced. It is also worth investigating whether these assumptions are reasonable.

ACKNOWLEDGMENTS

We thank P. Liu, X.-Y. Cao and C.-X. Weng for their valuable discussions. This work was supported by the Natural Science Foundation of Jiangsu Province (No. BK20211145), the Fundamental Research Funds for the Central Universities (No. 020414380182), the Key Research and Development Program of Nanjing Jiangbei New Area (No. ZDYD20210101), the Program for Innovative Talents and Entrepreneurs in Jiangsu (No. JSS-CRC2021484).

Appendix A: Post-processing.

Bob is a virtual party who thinks that the source is sending $|0\rangle_x$, and we can take Bob as a classical party for simplicity. To bound $H_{\max}^\epsilon(\mathbf{X}_A|\mathbf{B})$, we should evaluate the conflict between the guesses of Bob and the measurement outcomes of Alice in the \mathbb{X} basis. This entropy formula concerns the outcomes that we suppose to use the \mathbb{X} basis to measure signals that have actually been measured in \mathbb{Z} . Although we cannot obtain the outcomes directly, we can evaluate the probability that Bob guessed incorrectly by randomly choosing several rounds to test the outcome distribution in \mathbb{X} . This is why we introduce the monitoring basis \mathbb{X} , and the bit error rate $e_x = N_x^e/N_x$ reflects the probability that Bob guessed incorrectly in the asymptotic regime. When considering the finite-key effect, we can apply the random sampling method to e_x and obtain the upper bound $\bar{e}_x = e_x + \gamma(N_z, N_x, e_x, \epsilon_{rand})$ in the signals measured in

\mathbb{Z} with failure probability ϵ_{rand} , where γ is a fluctuation that can be numerically determined [59].

Furthermore, only the single-click events in \mathbb{Z} are valid random numbers. Other events, such as multiple-click events and no-click events, have no extractable randomness. The upper bound of probabilities of error rate in these single-click rounds [48] is $\bar{\phi}_z = (\bar{e}_x \times N_z)/N_z^s$, which means that all errors occurred in single-click events.

The smooth entropy $H_{\max}^\epsilon(\mathbf{X}_A|\mathbf{B})$ is defined as $h_d(\bar{\phi}_z)$, where $h_d(x) = -x \log_2(x/(d-1)) - (1-x) \log_2(1-x)$ is the Shannon entropy function [60, 61] in the case of d -dimensionality. The entropy $h_d(x)$ is concave and reaches its maximum value of $\log_2 d$ at $x = (d-1)/d$. When x is greater than $(d-1)/d$, i.e., the error rate is higher than that of random guesses, $H_{\max}^\epsilon(\mathbf{X}_A|\mathbf{B})$ is set to $\log_2 d$.

In two-dimensional measurement, $H_{\max}^\epsilon(\mathbf{X}_A|\mathbf{B})$ reduces to the binary Shannon entropy function $h_2(x) = -x \log_2(x) - (1-x) \log_2(1-x)$ with error rate x . The entropy $h_2(x)$ reaches its maximum value of 1 at $e_x = 0.5$. When x is greater than 0.5, we set $H_{\max}^\epsilon(\mathbf{X}_A|\mathbf{B}) = 1$.

Appendix B: Composable security against coherent attacks.

The uncertainty relation of smooth entropy shows the ability of generating randomness against coherent attacks [50, 51]. Additionally, we need the leftover hashing method [62] to distill random numbers from the randomness. For random number generation tasks, we focus on the secrecy in the composable security. In our protocol, there are three components that contribute to the secrecy: the smooth entropy, the random sampling fluctuation and the leftover hashing. They all have probabilities of failure. The failure probabilities of these components are labeled ϵ , ϵ_{rand} and ϵ_{hash} , respectively. According to the composable security, the protocol has ϵ_{sec} -secrecy when $\epsilon_{sec} \geq \epsilon + \epsilon_{rand} + \epsilon_{hash}$. For simplicity, we take $\epsilon = \epsilon_{rand} = \epsilon_{hash} = \epsilon_{sec}/3$. Through leftover hashing, we can generate a random number string of length ℓ :

$$\begin{aligned} \frac{1}{2} \sqrt{2^{\ell - H_{\min}^\epsilon(\mathbf{Z}_A|\mathbf{E})}} &\leq \epsilon_{hash}, \\ \ell &\geq H_{\min}^\epsilon(\mathbf{Z}_A|\mathbf{E}) - 2 \log_2 \frac{1}{2\epsilon_{hash}}. \end{aligned} \quad (\text{B1})$$

In accordance with Eq. (1), we finally obtain the length formula given in Eq. (F1).

Appendix C: Simulation.

In the text, we simulate the generation rates under different experimental conditions. The equations for simulation are shown below. In the simulation, we assume that the states are coherent states. The yield when the signal contains n photons and the measurement in \mathbb{X} causes a single click on the $|0\rangle_x$ detector is

$Y_n^{(0)x} = (1 - p_d)^{d-1} - (1 - p_d)^d(1 - \eta)^n$, where d is the dimensionality of measurement, p_d is the dark count and η evaluates the total loss, including the detection inefficiency. The gain of this kind of single-click event is $Q_\mu^x = (1 - p_d)^{d-1} - (1 - p_d)^d e^{-\mu'}$. Here, we can consider the light intensity and loss collectively as $\mu' = \mu\eta$, since both of them are insecure. The experiment indicates that the misalignment error is $e_d = 0.004$. We roughly use $N_x^e = N_x(1 - Q_\mu^x + e_d Q_\mu^x)$.

The yield when the signal contains n photons and the measurement in \mathbb{Z} causes a single click on one detector is $Y_n^{sc} = (1 - p_d)^{d-1} [(1 - (d-1)\eta/d)^n - (1 - \eta)^n(1 - p_d)]$. The gain of all single click events is $Q_\mu^z = d(1 - p_d)^{d-1} e^{-(d-1)\mu'/d} - d(1 - p_d)^d e^{-\mu'}$. We have $N_z^s = N_z Q_\mu^z$.

Appendix D: Calibration.

In experiments, the value of q should be calibrated. According to the entropy uncertainty relation, $q = -\log_2 \max_{x,z} |\langle x|z \rangle|^2$ is the incompatibility between two measurement bases. To realize the calibration, we first modify the light until the ratio of photon counts between the two detection channels is above 24 dB in the \mathbb{X} basis. This means that the light is approximately a perfect eigenstate of \mathbb{X} . Subsequently, we measure the light in the \mathbb{Z} basis and obtain the ratio of photon counts between the two detection channels. By comparing the single-click events in the two detection channels, the value of q is calibrated to $q = 0.954$ in our detection equipment.

The unbalanced detection efficiency should be taken into account. Its impact is introduced as a coefficient of the generation rate. This coefficient is $\eta_e = 2 \min\{(\eta_0, \eta_1)\} / (\eta_0 + \eta_1)$, which depends on the efficiencies of the two detection channels. The final random number extracted is

$$\ell \geq \eta_e \left(N_z^s [q - h_d(\bar{\phi}_z)] - 2 \log_2 \frac{3}{2\varepsilon_{\text{sec}}} \right) - n_{\text{seeds}}, \quad (\text{D1})$$

The detection efficiencies are 49% and 39%, respectively, in calibration. After taking the insert loss circulator (1.05 dB) into account, η_e is calculated to be 0.9932.

Appendix E: Random number consumption.

For the active-basis-choice, we need to consume some random numbers while generating them. First, the basis choice consumes approximately $N_x \log_2 N$ [25]. Second, we should assign the detection channel for measuring the eigenstate $|+\rangle$ every time we measure the state in \mathbb{X} . This consumes approximately $N_x \log_2 d$, where d is the dimensionality of the measurement. Therefore, the term n_{seeds} in Eqs. (F1) and (D1) is $n_{\text{seeds}} = N_x \log_2 N + N_x \log_2 d$.

Appendix F: SI-QRNG protocol treating no-click events as vacua

In the main text, we provide our protocol that resists detector blinding attacks by treating no-click events as error events. Previous SI-QRNG protocols did not consider detector blinding attacks, so they used squashing models to mark the no-click event as a vacuum. Since the vacuum cannot carry information and will not reveal information, they discard no-click events without hesitation. We compare the random number generation rate of our protocol and this kind of protocol. The rate difference implies the security risks caused by the detector blinding attack. To avoid the influence of different squashing model choices and the inconsistency of security parameters under different security frameworks, we use the following protocol as the representative of previous SI-QRNGs.

1. Protocol description

State preparation. Alice prepares signals that allow the detector representing $|+\rangle$ to fire. She sends N signals and does not trust the quantum states she prepared. Virtual party Bob guesses that the outcomes of measuring signals in \mathbb{X} basis are always $|+\rangle$.

Two-dimensional measurement. Alice randomly measures signals in basis \mathbb{X} or \mathbb{Z} with probability p_x and $p_z = 1 - p_x$, respectively. The no-click events are discarded.

Post-processing. Alice only deals with the click events. In the \mathbb{X} basis, the click events can be divided into two parts: n_x^c and n_x^e . n_x^c is the number of correct events that only the $|+\rangle$ detector fires. Other events, including double-click events and single-click events on the $|-\rangle$ detector, are considered as error results and counted into n_x^e . The error rate is $e_x = n_x^e / n_x$, where n_x is the number of click events in \mathbb{X} . In \mathbb{Z} , we care only about the single click results n_z^s of all n_z click events. According to the uncertainty relation of entropy, the length of secret random numbers with ε_{sec} -secrecy is given by

$$\ell \geq n_z^s [q - h_d(\bar{\phi}_z)] - 2 \log_2 \frac{3}{2\varepsilon_{\text{sec}}} - n_{\text{seeds}}, \quad (\text{F1})$$

where $\bar{\phi}_z = \frac{(e_x + \gamma(n_z, n_x, e_x, \epsilon_{\text{rand}})) \times n_z}{n_z^s}$ is the upper bound of the phase error rate in \mathbb{Z} , h_d is the d -dimensional Shannon entropy, and q is the incompatibility between two measurement bases. The active basis choice consumes some random seeds $n_{\text{seeds}} = N p_x \log_2 N$.

2. Simulation

In simulation, we assume that the states are coherent states. In the \mathbb{X} basis, the gain of click events is $Q_x = 1 - (1 - p_d)^2 e^{-\mu\eta}$, where p_d is the dark count, μ is the

intensity of light and η is the transmission efficiency. The number of click events is $n_x = Np_xQ_x$. The gain of error events is $Q_x^e = p_d + e_d(Q_x - p_d)$, where e_d is the misalignment error. The error rate is $e_x = Q_x^e/Q_x$.

In the \mathbb{Z} basis, the gain of click events is also $Q_z = 1 - (1 - p_d)^2 e^{-\mu\eta}$. The number of click events is $n_z = Np_zQ_z$. The gain of all single-click events is $Q_z^s = 2(1 - p_d)e^{-\mu\eta/2} - 2(1 - p_d)^2 e^{-\mu\eta}$. The number of single-click events is $n_z^s = Np_zQ_z^s$.

Appendix G: Detailed experimental results

In Tab. II, III, IV, V and VI we report the detailed results obtained in the experiment. In all the tables, we report the random number generation rate $R := \ell/N$, the number of time windows that Alice choose to measure in $Z(X)$ basis $N_{Z(X)}$, the total number of click events in detector D_H (D_V) in the Z basis, the number of single click events in detector D_H (D_V) in the Z basis, the error rate in the X basis e_x and the upper bound of phase error rate in the Z basis ϕ_z .

-
- [1] F. James, A review of pseudorandom number generators, *Comput. Phys. Commun.* **60**, 329 (1990).
 - [2] P. L'Ecuyer, Random number generation, in *Handbook of Computational Statistics: Concepts and Methods* (Springer, 2012) pp. 35–71.
 - [3] V. Fischer and M. Drutarovský, True random number generator embedded in reconfigurable hardware, in *Cryptographic Hardware and Embedded Systems - CHES 2002* (Springer, 2003) pp. 415–430.
 - [4] I. Reidler, Y. Aviad, M. Rosenbluh, and I. Kanter, Ultrahigh-speed random number generation based on a chaotic semiconductor laser, *Phys. Rev. Lett.* **103**, 024102 (2009).
 - [5] X. Ma, X. Yuan, Z. Cao, B. Qi, and Z. Zhang, Quantum random number generation, *npj Quantum Inf.* **2**, 1 (2016).
 - [6] M. Herrero-Collantes and J. C. Garcia-Escartin, Quantum random number generators, *Rev. Mod. Phys.* **89**, 015004 (2017).
 - [7] J. Liu, Y. Qi, Z. Y. Meng, and L. Fu, Self-learning monte carlo method, *Phys. Rev. B* **95**, 041101 (2017).
 - [8] N. Masuda, M. A. Porter, and R. Lambiotte, Random walks and diffusion on networks, *Phys. Rep.* **716-717**, 1 (2017).
 - [9] M.-O. Renou, D. Trillo, M. Weilenmann, T. P. Le, A. Tavakoli, N. Gisin, A. Acín, and M. Navascués, Quantum theory based on real numbers can be experimentally falsified, *Nature* **600**, 625 (2021).
 - [10] H.-L. Yin, Y. Fu, and Z.-B. Chen, Practical quantum digital signature, *Phys. Rev. A* **93**, 032316 (2016).
 - [11] P. Alikhani, N. Brunner, C. Crépeau, S. Designolle, R. Houlmann, W. Shi, N. Yang, and H. Zbinden, Experimental relativistic zero-knowledge proofs, *Nature* **599**, 47 (2021).
 - [12] Y. Fu, H.-L. Yin, T.-Y. Chen, and Z.-B. Chen, Long-distance measurement-device-independent multi-party quantum communication, *Phys. Rev. Lett.* **114**, 090501 (2015).
 - [13] S. Pirandola, U. L. Andersen, L. Banchi, M. Berta, D. Bunandar, R. Colbeck, D. Englund, T. Gehring, C. Lupo, C. Ottaviani, *et al.*, Advances in quantum cryptography, *Adv. Opt. Photon.* **12**, 1012 (2020).
 - [14] W.-B. Liu, C.-L. Li, Y.-M. Xie, C.-X. Weng, J. Gu, X.-Y. Cao, Y.-S. Lu, B.-H. Li, H.-L. Yin, and Z.-B. Chen, Homodyne detection quadrature phase shift keying continuous-variable quantum key distribution with high excess noise tolerance, *PRX Quantum* **2**, 040334 (2021).
 - [15] S. Pironio, A. Acín, S. Massar, A. B. de La Giroday, D. N. Matsukevich, P. Maunz, S. Olmschenk, D. Hayes, L. Luo, T. A. Manning, *et al.*, Random numbers certified by bell's theorem, *Nature* **464**, 1021 (2010).
 - [16] Y. Liu, Q. Zhao, M.-H. Li, J.-Y. Guan, Y. Zhang, B. Bai, W. Zhang, W.-Z. Liu, C. Wu, X. Yuan, *et al.*, Device-independent quantum random-number generation, *Nature* **562**, 548 (2018).
 - [17] Y. Zhang, L. K. Shalm, J. C. Bienfang, M. J. Stevens, M. D. Mazurek, S. W. Nam, C. Abellán, W. Amaya, M. W. Mitchell, H. Fu, C. A. Miller, A. Mink, and E. Knill, Experimental low-latency device-independent quantum randomness, *Phys. Rev. Lett.* **124**, 010505 (2020).
 - [18] P. Bierhorst, E. Knill, S. Glancy, Y. Zhang, A. Mink, S. Jordan, A. Rommal, Y.-K. Liu, B. Christensen, S. W. Nam, *et al.*, Experimentally generated randomness certified by the impossibility of superluminal signals, *Nature* **556**, 223 (2018).
 - [19] M.-H. Li, X. Zhang, W.-Z. Liu, S.-R. Zhao, B. Bai, Y. Liu, Q. Zhao, Y. Peng, J. Zhang, Y. Zhang, W. J. Munro, X. Ma, Q. Zhang, J. Fan, and J.-W. Pan, Experimental realization of device-independent quantum randomness expansion, *Phys. Rev. Lett.* **126**, 050503 (2021).
 - [20] L. K. Shalm, Y. Zhang, J. C. Bienfang, C. Schlager, M. J. Stevens, M. D. Mazurek, C. Abellán, W. Amaya, M. W. Mitchell, M. A. Alhejji, *et al.*, Device-independent randomness expansion with entangled photons, *Nat. Phys.* **17**, 452 (2021).
 - [21] W.-Z. Liu, M.-H. Li, S. Ragy, S.-R. Zhao, B. Bai, Y. Liu, P. J. Brown, J. Zhang, R. Colbeck, J. Fan, *et al.*, Device-independent randomness expansion against quantum side information, *Nat. Phys.* **17**, 448 (2021).
 - [22] Y. Zhang, H.-P. Lo, A. Mink, T. Ikuta, T. Honjo, H. Takesue, and W. J. Munro, A simple low-latency real-time certifiable quantum random number generator, *Nat. Commun.* **12**, 1056 (2021).
 - [23] A. Tavakoli, Semi-device-independent framework based on restricted distrust in prepare-and-measure experiments, *Phys. Rev. Lett.* **126**, 210503 (2021).
 - [24] Y.-Q. Nie, J.-Y. Guan, H. Zhou, Q. Zhang, X. Ma, J. Zhang, and J.-W. Pan, Experimental measurement-device-independent quantum random-number generation, *Phys. Rev. A* **94**, 060301 (2016).
 - [25] Z. Cao, H. Zhou, X. Yuan, and X. Ma, Source-independent quantum random number generation, *Phys. Rev. X* **6**, 011020 (2016).

- [26] D. G. Marangon, G. Vallone, and P. Villoresi, Source-device-independent ultrafast quantum random number generation, *Phys. Rev. Lett.* **118**, 060503 (2017).
- [27] M. Avesani, D. G. Marangon, G. Vallone, and P. Villoresi, Source-device-independent heterodyne-based quantum random number generator at 17 gbps, *Nat. Commun.* **9**, 5365 (2018).
- [28] D. Drahi, N. Walk, M. J. Hoban, A. K. Fedorov, R. Shakhovoy, A. Feimov, Y. Kurochkin, W. S. Kolthammer, J. Nunn, J. Barrett, and I. A. Walmsley, Certified quantum random numbers from untrusted light, *Phys. Rev. X* **10**, 041048 (2020).
- [29] T. Gehring, C. Lupo, A. Kordts, D. Solar Nikolic, N. Jain, T. Rydberg, T. B. Pedersen, S. Pirandola, and U. L. Andersen, Homodyne-based quantum random number generator at 2.9 gbps secure against quantum side-information, *Nat. Commun.* **12**, 605 (2021).
- [30] J. Cheng, J. Qin, S. Liang, J. Li, Z. Yan, X. Jia, and K. Peng, Mutually testing source-device-independent quantum random number generator, *Photonics Res.* **10**, 646 (2022).
- [31] F. Xu, X. Ma, Q. Zhang, H.-K. Lo, and J.-W. Pan, Secure quantum key distribution with realistic devices, *Rev. Mod. Phys.* **92**, 025002 (2020).
- [32] Y.-H. Li, X. Han, Y. Cao, X. Yuan, Z.-P. Li, J.-Y. Guan, Y. Yin, Q. Zhang, X. Ma, C.-Z. Peng, and J.-W. Pan, Quantum random number generation with uncharacterized laser and sunlight, *npj Quantum Inf.* **5**, 97 (2019).
- [33] X. Lin, S. Wang, Z.-Q. Yin, G.-J. Fan-Yuan, R. Wang, W. Chen, D.-Y. He, Z. Zhou, G.-C. Guo, and Z.-F. Han, Security analysis and improvement of source independent quantum random number generators with imperfect devices, *npj Quantum Inf.* **6**, 100 (2020).
- [34] L. Lydersen, C. Wiechers, C. Wittmann, D. Elser, J. Skaar, and V. Makarov, Hacking commercial quantum cryptography systems by tailored bright illumination, *Nat. Photonics* **4**, 686 (2010).
- [35] C. Wiechers, L. Lydersen, C. Wittmann, D. Elser, J. Skaar, C. Marquardt, V. Makarov, and G. Leuchs, After-gate attack on a quantum cryptosystem, *New J. Phys.* **13**, 013043 (2011).
- [36] L. Lydersen, N. Jain, C. Wittmann, Ø. Marøy, J. Skaar, C. Marquardt, V. Makarov, and G. Leuchs, Superlinear threshold detectors in quantum cryptography, *Phys. Rev. A* **84**, 032320 (2011).
- [37] I. Gerhardt, Q. Liu, A. Lamas-Linares, J. Skaar, C. Kurtstiefer, and V. Makarov, Full-field implementation of a perfect eavesdropper on a quantum cryptography system, *Nat. Commun.* **2**, 349 (2011).
- [38] L. Lydersen, M. K. Akhlaghi, A. H. Majedi, J. Skaar, and V. Makarov, Controlling a superconducting nanowire single-photon detector using tailored bright illumination, *New J. Phys.* **13**, 113042 (2011).
- [39] Z. Yuan, J. F. Dynes, and A. J. Shields, Avoiding the blinding attack in qkd, *Nat. Photonics* **4**, 800 (2010).
- [40] Y.-J. Qian, D.-Y. He, S. Wang, W. Chen, Z.-Q. Yin, G.-C. Guo, and Z.-F. Han, Robust countermeasure against detector control attack in a practical quantum key distribution system, *Optica* **6**, 1178 (2019).
- [41] M. Fujiwara, T. Honjo, K. Shimizu, K. Tamaki, and M. Sasaki, Characteristics of superconducting single photon detector in dps-qkd system under bright illumination blinding attack, *Opt. Express* **21**, 6304 (2013).
- [42] C. C. W. Lim, N. Walenta, M. Legré, N. Gisin, and H. Zbinden, Random variation of detector efficiency: A countermeasure against detector blinding attacks for quantum key distribution, *IEEE J. Sel. Top. Quantum Electron.* **21**, 192 (2015).
- [43] G. Gras, D. Rusca, H. Zbinden, and F. Bussi eres, Countermeasure against quantum hacking using detection statistics, *Phys. Rev. Applied* **15**, 034052 (2021).
- [44] Z. Wu, A. Huang, X. Qiang, J. Ding, P. Xu, X. Fu, and J. Wu, Robust countermeasure against detector control attack in a practical quantum key distribution system: comment, *Optica* **7**, 1391 (2020).
- [45] S. Sajeed, A. Huang, S. Sun, F. Xu, V. Makarov, and M. Curty, Insecurity of detector-device-independent quantum key distribution, *Phys. Rev. Lett.* **117**, 250505 (2016).
- [46] N. Brunner, D. Cavalcanti, S. Pironio, V. Scarani, and S. Wehner, Bell nonlocality, *Rev. Mod. Phys.* **86**, 419 (2014).
- [47] N. J. Beaudry, T. Moroder, and N. L utkenhaus, Squashing models for optical measurements in quantum communication, *Phys. Rev. Lett.* **101**, 093601 (2008).
- [48] C.-H. F. Fung, H. F. Chau, and H.-K. Lo, Universal squash model for optical communications using linear optics and threshold detectors, *Phys. Rev. A* **84**, 020303 (2011).
- [49] O. Gittsovich, N. J. Beaudry, V. Narasimhachar, R. R. Alvarez, T. Moroder, and N. L utkenhaus, Squashing model for detectors and applications to quantum-key-distribution protocols, *Phys. Rev. A* **89**, 012325 (2014).
- [50] M. Tomamichel and R. Renner, Uncertainty relation for smooth entropies, *Phys. Rev. Lett.* **106**, 110506 (2011).
- [51] M. Tomamichel, C. C. W. Lim, N. Gisin, and R. Renner, Tight finite-key analysis for quantum cryptography, *Nat. Commun.* **3**, 634 (2012).
- [52] H.-W. Li, S. Wang, J.-Z. Huang, W. Chen, Z.-Q. Yin, F.-Y. Li, Z. Zhou, D. Liu, Y. Zhang, G.-C. Guo, W.-S. Bao, and Z.-F. Han, Attacking a practical quantum-key-distribution system with wavelength-dependent beam-splitter and multiwavelength sources, *Phys. Rev. A* **84**, 062308 (2011).
- [53] P. V. P. Pinheiro, P. Chaiwongkhot, S. Sajeed, R. T. Horn, J.-P. Bourgoin, T. Jennewein, N. L utkenhaus, and V. Makarov, Eavesdropping and countermeasures for backflash side channel in quantum cryptography, *Opt. Express* **26**, 21020 (2018).
- [54] H.-L. Yin, P. Liu, W.-W. Dai, Z.-H. Ci, J. Gu, T. Gao, Q.-W. Wang, and Z.-Y. Shen, Experimental composable security decoy-state quantum key distribution using time-phase encoding, *Opt. Express* **28**, 29479 (2020).
- [55] Y. Zhao, C.-H. F. Fung, B. Qi, C. Chen, and H.-K. Lo, Quantum hacking: Experimental demonstration of time-shift attack against practical quantum-key-distribution systems, *Phys. Rev. A* **78**, 042333 (2008).
- [56] H. Weier, H. Krauss, M. Rau, M. F urst, S. Nauerth, and H. Weinfurter, Quantum eavesdropping without interception: an attack exploiting the dead time of single-photon detectors, *New J. Phys.* **13**, 073024 (2011).
- [57] A. Rukhin, J. Soto, J. Nechvatal, M. Smid, and E. Barker, *A statistical test suite for random and pseudorandom number generators for cryptographic applications*, Tech. Rep. (Booz-allen and hamilton inc mclean va, 2001).

- [58] W. Zhang, J. Huang, C. Zhang, L. You, C. Lv, L. Zhang, H. Li, Z. Wang, and X. Xie, A 16-pixel interleaved superconducting nanowire single-photon detector array with a maximum count rate exceeding 1.5 ghz, *IEEE Trans. Appl. Supercond.* **29**, 1 (2019).
- [59] H.-L. Yin, M.-G. Zhou, J. Gu, Y.-M. Xie, Y.-S. Lu, and Z.-B. Chen, Tight security bounds for decoy-state quantum key distribution, *Sci. Rep.* **10**, 14312 (2020).
- [60] Y. Ding, D. Bacco, K. Dalgaard, X. Cai, X. Zhou, K. Rottwitt, and L. K. Oxenløwe, High-dimensional quantum key distribution based on multicore fiber using silicon photonic integrated circuits, *npj Quantum Inf.* **3**, 25 (2017).
- [61] N. T. Islam, C. C. W. Lim, C. Cahall, J. Kim, and D. J. Gauthier, Provably secure and high-rate quantum key distribution with time-bin qudits, *Sci. Adv.* **3**, e1701491 (2017).
- [62] M. Tomamichel, C. Schaffner, A. Smith, and R. Renner, Leftover hashing against quantum side information, *IEEE Trans. Inf. Theory* **57**, 5524 (2011).

Intensity μ	6.32	6.8	7.7	9.6	14.3	18.2
R	0.0531	0.0761	0.0907	0.1010	0.0509	0
N_Z	1064540311	1059470000	999500000	1009708496	99549664	999511985
N_X	532592	530089	500049	505161	500078	500063
Total D_H click in the Z basis	732490456	795307879	792392154	860099255	939175515	968019162
Total D_V click in the Z basis	722825567	750713996	748852702	835145639	919880879	954610805
Single D_H click in the Z basis	235037676	232246534	198791921	148663349	74850323	43486700
Single D_V click in the Z basis	225372787	187652651	155252469	123709733	55555687	30078343
e_x	10.11%	7.69%	5.74%	2.99%	1.10%	2.19%
ϕ_z	23.95%	19.96%	16.76%	11.65%	9.17%	31.49%

TABLE II. Experiment results obtained for various pulse intensities.

Channel loss (dB)	0	1	3	10
R	0.0979	0.0839	0	0
N_Z	1009530770	1149424997	999592872	1229842581
N_X	505067	575054	500083	615245
Total D_H click in the Z basis	826646616	844496091	576423481	143298859
Total D_V click in the Z basis	849768774	861501605	566073702	136472595
Single D_H click in the Z basis	130668741	211532227	249937412	127373092
Single D_V click in the Z basis	153790899	228537741	239587633	120546828
e_x	3.42%	6.91%	19.64%	78.55%
ϕ_z	12.68%	18.57%	40.78%	50%

TABLE III. Experiment results obtained for various channel losses with a fixed intensity.

Channel loss (dB)	1	3	10
R	0.0959	0.0938	0.0995
N_Z	999980222	1009494998	1009882327
N_X	500292	505052	505248
Total D_H click in the Z basis	850571844	822977603	828712721
Total D_V click in the Z basis	835192945	851910282	842746871
Single D_H click in the Z basis	140183635	128031450	137373945
Single D_V click in the Z basis	124804736	156964129	151408095
e_x	3.04%	3.58%	3.47%
ϕ_z	12.05%	13.24%	12.69%

TABLE IV. Experiment results obtained for various channel losses with the optimal intensity.

Channel loss (dB)	0	1	3	10
R	0.220	0.319	0.387	0.171
N_Z	1009530770	1149424997	999592872	1229842581
N_X	505067	575054	500083	615245
Total D_H click in the Z basis	826646616	844496091	576423481	143298859
Total D_V click in the Z basis	849768774	861501605	566073702	136472595
Single D_H click in the Z basis	130668741	211532227	249937412	127373092
Single D_V click in the Z basis	153790899	228537741	239587633	120546828
e_x	0.41%	0.36%	1.01%	0.20%
ϕ_z	1.62%	1.02%	1.86%	0.32%

TABLE V. Experiment results obtained for various channel losses with a fixed intensity, used for the protocol in Appendix.

R	0.103
N_Z	1015527087
N_X	508128
Total D_H click in the Z basis	854697340
Total D_V click in the Z basis	824303459
Single D_H click in the Z basis	160570766
Single D_V click in the Z basis	130176885
e_x	3.34%
$\overline{\phi}_z$	12.2%

TABLE VI. Experimental results used for final random number generation.